Pion Multiplet Spectrum with Improved Staggered Fermions

David H. Adams[1], Taegil Bae[1], Chulwoo Jung[2], Hyung-Jin Kim[1], Jongjeong Kim[1], Kwangwoo Kim[1], Weonjong Lee[1], and Stephen R. Sharpe[3]

[1]Department of Physics and Astronomy, Seoul National University
[2]Physics Department, Brookhaven National Laboratory
[3]Physics Department, University of Washington

Nuclear and Particle Physics Session, HPC Asia 2007, Seoul

Outline

Outline

Outline

Outline

1. Introduction to Lattice QCD
   - Why Lattice QCD?
   - Elements of Lattice QCD
2. Pion Multiplet Spectrum in Staggered Fermions
   - Staggered Fermions
   - Spectroscopy
   - Analysis
   - Simulation Parameters
   - Results
3. Conclusion

Quantum Chromodynamics(QCD)

QCD is a theory of the strong interactions of hadrons, with quarks and gluons as the fundamental particles. It is a non-abelian gauge theory and has the following properities.

- Confinement
  Quarks and gluons are forever bound into hadrons.
- Asymptotic Freedom
  At short distance(high energy scale), the interaction is so weak that perturbative methods work. The asymptotic freedom implies that at long distance the interaction becomes stronger, thus perturbative methods do not work.

Therefore

We need non-perturbative methods to study the low energy physics of QCD.

Quantum Chromodynamics(QCD)

QCD is a theory of the strong interactions of hadrons, with quarks and gluons as the fundamental particles. It is a non-abelian gauge theory and has the following properities.

- Confinement
  Quarks and gluons are forever bound into hadrons.
- Asymptotic Freedom
  At short distance(high energy scale), the interaction is so weak that perturbative methods work. The asymptotic freedom implies that at long distance the interaction becomes stronger, thus perturbative methods do not work.

Therefore

We need non-perturbative methods to study the low energy physics of QCD.

Quantum Chromodynamics(QCD)

QCD is a theory of the strong interactions of hadrons, with quarks and gluons as the fundamental particles. It is a non-abelian gauge theory and has the following properities.

- Confinement
  Quarks and gluons are forever bound into hadrons.
- Asymptotic Freedom
  At short distance(high energy scale), the interaction is so weak that perturbative methods work. The asymptotic freedom implies that at long distance the interaction becomes stronger, thus perturbative methods do not work.

Therefore

We need non-perturbative methods to study the low energy physics of QCD.

Quantum Chromodynamics(QCD)

QCD is a theory of the strong interactions of hadrons, with quarks and gluons as the fundamental particles. It is a non-abelian gauge theory and has the following properities.

- Confinement
  Quarks and gluons are forever bound into hadrons.
- Asymptotic Freedom
  At short distance(high energy scale), the interaction is so weak that perturbative methods work. The asymptotic freedom implies that at long distance the interaction becomes stronger, thus perturbative methods do not work.

Therefore

We need non-perturbative methods to study the low energy physics of QCD.

Lattice QCD

- Lattice QCD is the discretized version of QCD where the space-time is discretized into a grid.
- Lattice discretization provides a non-perturbative regularization scheme.
- Due to the analogy between Euclidean field theory and statistical mechanics system, lattice QCD can be simulated on the computer using methods of statistical mechanics.

Lattice QCD Calulation

Physical observables can be obtained by calculating expectation values.

$$\langle \mathcal{O} \rangle = \frac{1}{Z} \int \mathcal{D}A_\mu \mathcal{D}\psi \mathcal{D}\bar{\psi} \mathcal{O} e^{-S} \qquad (1)$$

Lattice QCD

- Lattice QCD is the discretized version of QCD where the space-time is discretized into a grid.
- Lattice discretization provides a non-perturbative regularization scheme.
- Due to the analogy between Euclidean field theory and statistical mechanics system, lattice QCD can be simulated on the computer using methods of statistical mechanics.

Lattice QCD Calulation

Physical observables can be obtained by calculating expectation values.

$$\langle \mathcal{O} \rangle = \frac{1}{Z} \int \mathcal{D}A_\mu \mathcal{D}\psi \mathcal{D}\bar{\psi} \mathcal{O} e^{-S} \quad (1)$$

Lattice QCD

- Lattice QCD is the discretized version of QCD where the space-time is discretized into a grid.
- Lattice discretization provides a non-perturbative regularization scheme.
- Due to the analogy between Euclidean field theory and statistical mechanics system, lattice QCD can be simulated on the computer using methods of statistical mechanics.

Lattice QCD Calulation

Physical observables can be obtained by calculating expectation values.

$$\langle \mathcal{O} \rangle = \frac{1}{Z} \int \mathcal{D}A_\mu \mathcal{D}\psi \mathcal{D}\bar{\psi} \mathcal{O} e^{-S} \quad (1)$$

Lattice QCD

- Lattice QCD is the discretized version of QCD where the space-time is discretized into a grid.
- Lattice discretization provides a non-perturbative regularization scheme.
- Due to the analogy between Euclidean field theory and statistical mechanics system, lattice QCD can be simulated on the computer using methods of statistical mechanics.

Lattice QCD Calulation

Physical observables can be obtained by calculating expectation values.

$$\langle \mathcal{O} \rangle = \frac{1}{Z} \int \mathcal{D}A_\mu \mathcal{D}\psi \mathcal{D}\bar{\psi} \mathcal{O} e^{-S} \quad (1)$$

Lattice QCD

- Lattice QCD is the discretized version of QCD where the space-time is discretized into a grid.
- Lattice discretization provides a non-perturbative regularization scheme.
- Due to the analogy between Euclidean field theory and statistical mechanics system, lattice QCD can be simulated on the computer using methods of statistical mechanics.

Lattice QCD Calulation

Physical observables can be obtained by calculating expectation values.

$$\langle \mathcal{O} \rangle = \frac{1}{Z} \int \mathcal{D}A_\mu \mathcal{D}\psi \mathcal{D}\bar{\psi} \mathcal{O} e^{-S} \quad (1)$$

Outline

Lattice Gauge Fields

The Continuum Pure Gauge Action

$$S_G = \int d^4x \frac{1}{4} F^a_{\mu\nu} F^a_{\mu\nu} \quad (2)$$

- While matter fields are put on lattice sites, gauge fields are put on links connecting two adjacent sites.
- Instead of gauge field $A_\mu(x)$, gauge group elements $U_\mu(x)$ are used.

Lattice Gauge Action (Wilson's Action)

$$S_G = \frac{2N}{g^2} \sum_x \sum_{\mu<\nu} \left(1 - \frac{1}{N} \mathrm{Re\ Tr} U_p\right) \quad (3)$$

Lattice Gauge Fields

The Continuum Pure Gauge Action

$$S_G = \int d^4x \frac{1}{4} F^a_{\mu\nu} F^a_{\mu\nu} \quad (2)$$

- While matter fields are put on lattice sites, gauge fields are put on links connecting two adjacent sites.
- Instead of gauge field $A_\mu(x)$, gauge group elements $U_\mu(x)$ are used.

Lattice Gauge Action (Wilson's Action)

$$S_G = \frac{2N}{g^2} \sum_x \sum_{\mu<\nu} (1 - \frac{1}{N} \mathrm{Re}\ \mathrm{Tr} U_p) \quad (3)$$

Lattice Gauge Fields

The Continuum Pure Gauge Action

$$S_G = \int d^4x \frac{1}{4} F^a_{\mu\nu} F^a_{\mu\nu} \tag{2}$$

- While matter fields are put on lattice sites, gauge fields are put on links connecting two adjacent sites.
- Instead of gauge field $A_\mu(x)$, gauge group elements $U_\mu(x)$ are used.

Lattice Gauge Action (Wilson's Action)

$$S_G = \frac{2N}{g^2} \sum_x \sum_{\mu<\nu} (1 - \frac{1}{N} \text{Re Tr} U_p) \tag{3}$$

Lattice Gauge Fields

The Continuum Pure Gauge Action

$$S_G = \int d^4x \frac{1}{4} F^a_{\mu\nu} F^a_{\mu\nu} \tag{2}$$

- While matter fields are put on lattice sites, gauge fields are put on links connecting two adjacent sites.
- Instead of gauge field $A_\mu(x)$, gauge group elements $U_\mu(x)$ are used.

Lattice Gauge Action (Wilson's Action)

$$S_G = \frac{2N}{g^2} \sum_x \sum_{\mu<\nu} (1 - \frac{1}{N} \mathrm{Re}\ \mathrm{Tr} U_p) \tag{3}$$

Lattice Fermions

- The naive discretization of fermion action results in species doubling.
- To overcome this, some lattice formulations of fermion action is developed.
  - Wilson fermions
  - Staggered fermions
  - Domain wall fermions
  - Overlap fermions
- Fermion fields are grassman variables. So the fermion part of the action is practically integrated out and contributes as a determinant of the fermion matrix.
  - Quenched QCD
  - Patially quenched QCD
  - Full QCD

Lattice Fermions

- The naive discretization of fermion action results in species doubling.
- To overcome this, some lattice formulations of fermion action is developed.
  - Wilson fermions
  - Staggered fermions
  - Domain wall fermions
  - Overlap fermions
- Fermion fields are grassman variables. So the fermion part of the action is practically integrated out and contributes as a determinant of the fermion matrix.
  - Quenched QCD
  - Patially quenched QCD
  - Full QCD

Lattice Fermions

- The naive discretization of fermion action results in species doubling.
- To overcome this, some lattice formulations of fermion action is developed.
    - Wilson fermions
    - Staggered fermions
    - Domain wall fermions
    - Overlap fermions
- Fermion fields are grassman variables. So the fermion part of the action is practically integrated out and contributes as a determinant of the fermion matrix.
    - Quenched QCD
    - Patially quenched QCD
    - Full QCD

Lattice Fermions

- The naive discretization of fermion action results in species doubling.
- To overcome this, some lattice formulations of fermion action is developed.
  - Wilson fermions
  - Staggered fermions
  - Domain wall fermions
  - Overlap fermions
- Fermion fields are grassman variables. So the fermion part of the action is practically integrated out and contributes as a determinant of the fermion matrix.
  - Quenched QCD
  - Patially quenched QCD
  - Full QCD

Outline

Staggered Fermions

Staggered Fermion Action

$$S_F = \frac{1}{2a}\sum_{x,\mu}\bar{\chi}(x)\eta_\mu(x)[U_\mu(x)\chi(x+\hat{\mu}) - U_\mu(x-\hat{\mu})^\dagger\chi(x-\hat{\mu})] + m\sum_x \bar{\chi}(x)\chi(x) \quad (4)$$

where $\eta_\mu(x) = (-1)^{\sum_{\nu<\mu} x_\nu}$.

- Staggered fermion field $\chi(x)$ is one-component field.
- One staggered fermion field corresponds to 4 degenerate fermions in continuum limit. We call these *taste*.
- At non-zero lattice spacing, the action has taste symmetry breaking terms.
- At zero quark mass, this action has the remnant chrial symmetry, $U(1)_A$. Spontaneous breaking of this symmetry results in a single Goldstone boson.

Staggered Fermions

Staggered Fermion Action

$$S_F = \frac{1}{2a}\sum_{x,\mu}\bar{\chi}(x)\eta_\mu(x)[U_\mu(x)\chi(x+\hat{\mu}) - U_\mu(x-\hat{\mu})^\dagger\chi(x-\hat{\mu})] + m\sum_x \bar{\chi}(x)\chi(x) \quad (4)$$

where $\eta_\mu(x) = (-1)^{\sum_{\nu<\mu} x_\nu}$.

- Staggered fermion field $\chi(x)$ is one-component field.
- One staggered fermion field corresponds to 4 degenerate fermions in continuum limit. We call these *taste*.
- At non-zero lattice spacing, the action has taste symmetry breaking terms.
- At zero quark mass, this action has the remnant chrial symmetry, $U(1)_A$. Spontaneous breaking of this symmetry results in a single Goldstone boson.

Staggered Fermions

Staggered Fermion Action

$$S_F = \frac{1}{2a}\sum_{x,\mu}\bar{\chi}(x)\eta_\mu(x)[U_\mu(x)\chi(x+\hat{\mu})-U_\mu(x-\hat{\mu})^\dagger\chi(x-\hat{\mu})]+m\sum_x\bar{\chi}(x)\chi(x) \quad (4)$$

where $\eta_\mu(x) = (-1)^{\sum_{\nu<\mu} x_\nu}$.

- Staggered fermion field $\chi(x)$ is one-component field.
- One staggered fermion field corresponds to 4 degenerate fermions in continuum limit. We call these *taste*.
- At non-zero lattice spacing, the action has taste symmetry breaking terms.
- At zero quark mass, this action has the remnant chrial symmetry, $U(1)_A$. Spontaneous breaking of this symmetry results in a single Goldstone boson.

Staggered Fermions

Staggered Fermion Action

$$S_F = \frac{1}{2a} \sum_{x,\mu} \bar{\chi}(x)\eta_\mu(x)[U_\mu(x)\chi(x+\hat{\mu}) - U_\mu(x-\hat{\mu})^\dagger \chi(x-\hat{\mu})] + m \sum_x \bar{\chi}(x)\chi(x) \quad (4)$$

where $\eta_\mu(x) = (-1)^{\sum_{\nu<\mu} x_\nu}$.

- Staggered fermion field $\chi(x)$ is one-component field.
- One staggered fermion field corresponds to 4 degenerate fermions in continuum limit. We call these *taste*.
- At non-zero lattice spacing, the action has taste symmetry breaking terms.
- At zero quark mass, this action has the remnant chrial symmetry, $U(1)_A$. Spontaneous breaking of this symmetry results in a single Goldstone boson.

Staggered Fermions

Staggered Fermion Action

$$S_F = \frac{1}{2a}\sum_{x,\mu}\bar{\chi}(x)\eta_\mu(x)[U_\mu(x)\chi(x+\hat{\mu}) - U_\mu(x-\hat{\mu})^\dagger\chi(x-\hat{\mu})] + m\sum_x \bar{\chi}(x)\chi(x) \tag{4}$$

where $\eta_\mu(x) = (-1)^{\sum_{\nu<\mu} x_\nu}$.

- Staggered fermion field $\chi(x)$ is one-component field.
- One staggered fermion field corresponds to 4 degenerate fermions in continuum limit. We call these *taste*.
- At non-zero lattice spacing, the action has taste symmetry breaking terms.
- At zero quark mass, this action has the remnant chrial symmetry, $U(1)_A$. Spontaneous breaking of this symmetry results in a single Goldstone boson.

Staggered Mesons

Staggered Meson in Spin-Taste Basis

$$O_{S,T} = \bar{\psi}(\gamma_S \otimes \xi_T)\psi \quad (5)$$

- The taste multiplicity leads to 16 multiplets of a pion. The pions have the spin-taste structure $(\gamma_5 \otimes \xi_T)$ with $\xi_T \in \{I, \xi_5, \xi_\mu, \xi_{\mu 5}, \xi_{\mu\nu} = \frac{1}{2}[\xi_\mu, \xi_\nu]\}$.
- These fall into 8 irreps of the lattice timeslice group, with tastes $\{I\}, \{\xi_5\}, \{\xi_i\}, \{\xi_4\}, \{\xi_{i5}\}, \{\xi_{45}\}, \{\xi_{ij}\}$, and $\{\xi_{i4}\}$.
- As a result of studies using staggered chiral perturbation theory, we expect that, to good approximation, the pions will lie in 5 irreps of SO(4) taste symmetry: $\{I\}, \{\xi_5\}, \{\xi_\mu\}, \{\xi_{\mu 5}\}, \{\xi_{\mu\nu}\}$.
- The pion with taste ξ_5 is the Goldstone pion.
- We compare Kluberg-Sten's operator and Golterman's one numerically.

Staggered Mesons

Staggered Meson in Spin-Taste Basis

$$O_{S,T} = \bar{\psi}(\gamma_S \otimes \xi_T)\psi \quad (5)$$

- The taste multiplicity leads to 16 multiplets of a pion. The pions have the spin-taste structure $(\gamma_5 \otimes \xi_T)$ with $\xi_T \in \{I, \xi_5, \xi_\mu, \xi_{\mu5}, \xi_{\mu\nu} = \frac{1}{2}[\xi_\mu, \xi_\nu]\}$.
- These fall into 8 irreps of the lattice timeslice group, with tastes $\{I\}, \{\xi_5\}, \{\xi_i\}, \{\xi_4\}, \{\xi_{i5}\}, \{\xi_{45}\}, \{\xi_{ij}\}$, and $\{\xi_{i4}\}$.
- As a result of studies using staggered chiral perturbation theory, we expect that, to good approximation, the pions will lie in 5 irreps of SO(4) taste symmetry: $\{I\}, \{\xi_5\}, \{\xi_\mu\}, \{\xi_{\mu5}\}, \{\xi_{\mu\nu}\}$.
- The pion with taste ξ_5 is the Goldstone pion.
- We compare Kluberg-Sten's operator and Golterman's one numerically.

Staggered Mesons

Staggered Meson in Spin-Taste Basis

$$O_{S,T} = \bar{\psi}(\gamma_S \otimes \xi_T)\psi \tag{5}$$

- The taste multiplicity leads to 16 multiplets of a pion. The pions have the spin-taste structure $(\gamma_5 \otimes \xi_T)$ with $\xi_T \in \{I, \xi_5, \xi_\mu, \xi_{\mu 5}, \xi_{\mu\nu} = \frac{1}{2}[\xi_\mu, \xi_\nu]\}$.
- These fall into 8 irreps of the lattice timeslice group, with tastes $\{I\}, \{\xi_5\}, \{\xi_i\}, \{\xi_4\}, \{\xi_{i5}\}, \{\xi_{45}\}, \{\xi_{ij}\},$ and $\{\xi_{i4}\}$.
- As a result of studies using staggered chiral perturbation theory, we expect that, to good approximation, the pions will lie in 5 irreps of SO(4) taste symmetry: $\{I\}, \{\xi_5\}, \{\xi_\mu\}, \{\xi_{\mu 5}\}, \{\xi_{\mu\nu}\}$.
- The pion with taste ξ_5 is the Goldstone pion.
- We compare Kluberg-Sten's operator and Golterman's one numerically.

Staggered Mesons

Staggered Meson in Spin-Taste Basis

$$O_{S,T} = \bar{\psi}(\gamma_S \otimes \xi_T)\psi \quad (5)$$

- The taste multiplicity leads to 16 multiplets of a pion. The pions have the spin-taste structure $(\gamma_5 \otimes \xi_T)$ with $\xi_T \in \{I, \xi_5, \xi_\mu, \xi_{\mu 5}, \xi_{\mu\nu} = \frac{1}{2}[\xi_\mu, \xi_\nu]\}$.
- These fall into 8 irreps of the lattice timeslice group, with tastes $\{I\}, \{\xi_5\}, \{\xi_i\}, \{\xi_4\}, \{\xi_{i5}\}, \{\xi_{45}\}, \{\xi_{ij}\}$, and $\{\xi_{i4}\}$.
- As a result of studies using staggered chiral perturbation theory, we expect that, to good approximation, the pions will lie in 5 irreps of SO(4) taste symmetry: $\{I\}, \{\xi_5\}, \{\xi_\mu\}, \{\xi_{\mu 5}\}, \{\xi_{\mu\nu}\}$.
- The pion with taste ξ_5 is the Goldstone pion.
- We compare Kluberg-Sten's operator and Golterman's one numerically.

Staggered Mesons

Staggered Meson in Spin-Taste Basis

$$O_{S,T} = \bar{\psi}(\gamma_S \otimes \xi_T)\psi \quad (5)$$

- The taste multiplicity leads to 16 multiplets of a pion. The pions have the spin-taste structure $(\gamma_5 \otimes \xi_T)$ with $\xi_T \in \{I, \xi_5, \xi_\mu, \xi_{\mu 5}, \xi_{\mu\nu} = \frac{1}{2}[\xi_\mu, \xi_\nu]\}$.
- These fall into 8 irreps of the lattice timeslice group, with tastes $\{I\}, \{\xi_5\}, \{\xi_i\}, \{\xi_4\}, \{\xi_{i5}\}, \{\xi_{45}\}, \{\xi_{ij}\}$, and $\{\xi_{i4}\}$.
- As a result of studies using staggered chiral perturbation theory, we expect that, to good approximation, the pions will lie in 5 irreps of SO(4) taste symmetry: $\{I\}, \{\xi_5\}, \{\xi_\mu\}, \{\xi_{\mu 5}\}, \{\xi_{\mu\nu}\}$.
- The pion with taste ξ_5 is the Goldstone pion.
- We compare Kluberg-Sten's operator and Golterman's one numerically.

Staggered Mesons

Staggered Meson in Spin-Taste Basis

$$O_{S,T} = \bar{\psi}(\gamma_S \otimes \xi_T)\psi \tag{5}$$

- The taste multiplicity leads to 16 multiplets of a pion. The pions have the spin-taste structure $(\gamma_5 \otimes \xi_T)$ with $\xi_T \in \{I, \xi_5, \xi_\mu, \xi_{\mu 5}, \xi_{\mu\nu} = \frac{1}{2}[\xi_\mu, \xi_\nu]\}$.
- These fall into 8 irreps of the lattice timeslice group, with tastes $\{I\}, \{\xi_5\}, \{\xi_i\}, \{\xi_4\}, \{\xi_{i5}\}, \{\xi_{45}\}, \{\xi_{ij}\}$, and $\{\xi_{i4}\}$.
- As a result of studies using staggered chiral perturbation theory, we expect that, to good approximation, the pions will lie in 5 irreps of SO(4) taste symmetry: $\{I\}, \{\xi_5\}, \{\xi_\mu\}, \{\xi_{\mu 5}\}, \{\xi_{\mu\nu}\}$.
- The pion with taste ξ_5 is the Goldstone pion.
- We compare Kluberg-Sten's operator and Golterman's one numerically.

Kluberg-Stern Operator

H. Kluberg-Stern *et al.*, NPB220 (1983) 447

Kluberg-Stern Meson Operator

$$O_{S,T}(t) = \sum_{\vec{n}} \sum_{A,B} \bar{\chi}(z+A)(\overline{\gamma_S \otimes \xi_T})_{A,B}\chi(z+B)$$

$$(\overline{\gamma_S \otimes \xi_T})_{A,B} = \frac{1}{4}\mathrm{Tr}(\gamma_A^\dagger \gamma_S \gamma_B \gamma_T^\dagger) \qquad (6)$$

where $z = (2\vec{n}, t)$ and A, B are vectors in the 2^4 hypercube.

- Simple, but approximate representations of the timeslice group.

Golterman Operator

M. Golterman, NPB273 (1986) 663

Golterman Meson Operator

$$O_{S,T}(t) = \sum_{\vec{x}} \Gamma_{S,T}(x)\bar{\chi}(x)\Omega_{S,T}\chi(x) \quad (7)$$

$$\Omega_{S,T}\chi(x) = \prod_{\mu=1,2,3} \left[(1 - |S_\mu - T_\mu|) + |S_\mu - T_\mu|\, \Phi_\mu\right] \chi(x) \quad (8)$$

$$\Phi_\mu \chi(x) = \frac{1}{2}\left[\chi(x+\hat{\mu}) + \chi(x-\hat{\mu})\right] \quad (9)$$

$\Gamma_{S,T}(x)$: phase factor given in NPB273 (1986) 663

- gives true irreps of the timeslice group.

Improved Staggered fermions

- The splitting between the pion multiplets are a non-perturbative measure of taste symmetry breaking, and can be used to measure the efficacy of different improvement schemes.
- It is known that fat link actions for staggered fermions reduce the taste symmetry breaking.
- In fat link actions, the original thin link variables $U_\mu(x)$ are replaced by a combination of extended gauge paths in a gauge invariant manner.
- We compare pion specturm splittings of HYP-smeared and AsqTad staggered fermions in unquenched QCD. We also compare HYP-smeared staggered fermions with unimproved staggered fermions in quenched QCD.

Improved Staggered fermions

- The splitting between the pion multiplets are a non-perturbative measure of taste symmetry breaking, and can be used to measure the efficacy of different improvement schemes.
- It is known that fat link actions for staggered fermions reduce the taste symmetry breaking.
- In fat link actions, the original thin link variables $U_\mu(x)$ are replaced by a combination of extended gauge paths in a gauge invariant manner.
- We compare pion specturm splittings of HYP-smeared and AsqTad staggered fermions in unquenched QCD. We also compare HYP-smeared staggered fermions with unimproved staggered fermions in quenched QCD.

Improved Staggered fermions

- The splitting between the pion multiplets are a non-perturbative measure of taste symmetry breaking, and can be used to measure the efficacy of different improvement schemes.
- It is known that fat link actions for staggered fermions reduce the taste symmetry breaking.
- In fat link actions, the original thin link variables $U_\mu(x)$ are replaced by a combination of extended gauge paths in a gauge invariant manner.
- We compare pion specturm splittings of HYP-smeared and AsqTad staggered fermions in unquenched QCD. We also compare HYP-smeared staggered fermions with unimproved staggered fermions in quenched QCD.

HYP Smearing

A. Hasenfratz & F. Knechtli, PRD64 (2001) 034504

- In continuum field theory, Dirac spinors $\Psi(x)$ couple to gauge fields $A_\mu(x)$ at the same local point x.
- Since Dirac components of each staggered quark $\psi(y)$ are distributed to different sites within a hypercube with its origin at y and each lattice site couples to different gauge fields.
- Thus the different flavor and Dirac components feel different gauge environments.
- Fattening links, in effect, smoothes the gauge fields so that it can remove some of the local fluctuations thus improving taste symmetry.
- HYP-smearing smoothes the gauge fields in the hypercubes attached to the original link.

HYP Smearing

A. Hasenfratz & F. Knechtli, PRD64 (2001) 034504

- In continuum field theory, Dirac spinors $\Psi(x)$ couple to gauge fields $A_\mu(x)$ at the same local point x.
- Since Dirac components of each staggered quark $\psi(y)$ are distributed to different sites within a hypercube with its origin at y and each lattice site couples to different gauge fields.
- Thus the different flavor and Dirac components feel different gauge environments.
- Fattening links, in effect, smoothes the gauge fields so that it can remove some of the local fluctuations thus improving taste symmetry.
- HYP-smearing smoothes the gauge fields in the hypercubes attached to the original link.

HYP Smearing

A. Hasenfratz & F. Knechtli, PRD64 (2001) 034504

- In continuum field theory, Dirac spinors $\Psi(x)$ couple to gauge fields $A_\mu(x)$ at the same local point x.
- Since Dirac components of each staggered quark $\psi(y)$ are distributed to different sites within a hypercube with its origin at y and each lattice site couples to different gauge fields.
- Thus the different flavor and Dirac components feel different gauge environments.
- Fattening links, in effect, smoothes the gauge fields so that it can remove some of the local fluctuations thus improving taste symmetry.
- HYP-smearing smoothes the gauge fields in the hypercubes attached to the original link.

HYP Smearing

A. Hasenfratz & F. Knechtli, PRD64 (2001) 034504

- In continuum field theory, Dirac spinors $\Psi(x)$ couple to gauge fields $A_\mu(x)$ at the same local point x.
- Since Dirac components of each staggered quark $\psi(y)$ are distributed to different sites within a hypercube with its origin at y and each lattice site couples to different gauge fields.
- Thus the different flavor and Dirac components feel different gauge environments.
- Fattening links, in effect, smoothes the gauge fields so that it can remove some of the local fluctuations thus improving taste symmetry.
- HYP-smearing smoothes the gauge fields in the hypercubes attached to the original link.

HYP Smearing

A. Hasenfratz & F. Knechtli, PRD64 (2001) 034504

- In continuum field theory, Dirac spinors $\Psi(x)$ couple to gauge fields $A_\mu(x)$ at the same local point x.
- Since Dirac components of each staggered quark $\psi(y)$ are distributed to different sites within a hypercube with its origin at y and each lattice site couples to different gauge fields.
- Thus the different flavor and Dirac components feel different gauge environments.
- Fattening links, in effect, smoothes the gauge fields so that it can remove some of the local fluctuations thus improving taste symmetry.
- HYP-smearing smoothes the gauge fields in the hypercubes attached to the original link.

HYP Smearing

A. Hasenfratz & F. Knechtli, PRD64 (2001) 034504

- In continuum field theory, Dirac spinors $\Psi(x)$ couple to gauge fields $A_\mu(x)$ at the same local point x.
- Since Dirac components of each staggered quark $\psi(y)$ are distributed to different sites within a hypercube with its origin at y and each lattice site couples to different gauge fields.
- Thus the different flavor and Dirac components feel different gauge environments.
- Fattening links, in effect, smoothes the gauge fields so that it can remove some of the local fluctuations thus improving taste symmetry.
- HYP-smearing smoothes the gauge fields in the hypercubes attached to the original link.

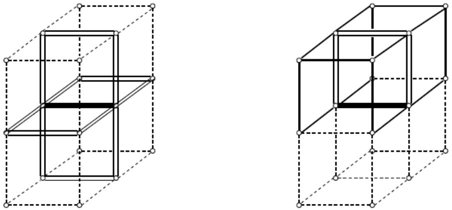

HYP Smearing

$$V_{i,\mu} = \text{Proj}_{SU(3)}[(1-\alpha_1)U_{i,\mu} + \frac{\alpha_1}{6}\sum_{\pm\nu\neq\mu} \tilde{V}_{i,\nu;\mu}\tilde{V}_{i+\hat{\nu},\mu;\nu}\tilde{V}^{\dagger}_{i,\nu;\mu}], \quad (10)$$

$$\tilde{V}_{i,\mu;\nu} = \text{Proj}_{SU(3)}[(1-\alpha_2)U_{i,\mu} + \frac{\alpha_2}{4}\sum_{\pm\rho\neq\nu,\mu} \bar{V}_{i,\rho;\nu\mu}\bar{V}_{i+\hat{\rho},\mu;\rho\nu}\bar{V}^{\dagger}_{i+\hat{\mu},\rho;\nu\mu}], \quad (11)$$

$$\bar{V}_{i,\mu;\nu\rho} = \text{Proj}_{SU(3)}[(1-\alpha_3)U_{i,\mu} + \frac{\alpha_3}{2}\sum_{\pm\eta\neq\rho,\nu,\mu} U_{i,\eta}U_{i+\hat{\eta},\mu}U^{\dagger}_{i+\hat{\mu},\eta}]. \quad (12)$$

AsqTad Action

G. P. Lepage, PRD59 (1999) 074502, K. Originos *et al.*, PRD60 (1999) 054503

- The tastes can be changed by one-gluon exchange with momentum $q \approx \zeta\pi/a$ where ζ is a vector with one or more components equal to 1 and all the others 0.
- This taste-changing interaction causes the taste symmetry breaking.
- In AsqTad action, one changes the quark-gluon coupling to suppress gluon momenta near $\zeta\pi/a$ for each of the ζ's.

AsqTad Action

$$\Delta_\mu \quad \rightarrow \quad \Delta'_\mu - \frac{a^2}{6}(\Delta_\mu)^3. \qquad (13)$$

In the Δ'_μ, U_μ are replaced by fattened links, while this is unnecessary in the Δ^3_μ term.

Outline

Mesonic Correlator

Correlator of Zero Momentum Flavor Non-Siglet Meson

$$\begin{aligned} C(t) &= \langle O(t)\bar{O}(0)\rangle \\ &= \sum_{\vec{x}} \langle \bar{\psi}^1(x)\Gamma\psi^2(x)\bar{\psi}^2(0)\Gamma\psi^1(0)\rangle \\ &= -\sum_{\vec{x}} \mathrm{Tr}[G(x,0)\Gamma G(0,x)\Gamma] \end{aligned} \tag{14}$$

- The propagator $G(x,0)$ is obtained by solving the Dirac equation with source $\delta(x)$.
- We however use cubic U(1) sources and cubic wall sources. Doing like this, we can get the lowest state in shorter time. Automatically we compare these two sources numerically.

Cubic U(1) Sources and Cubic Wall Sources

Cubic U(1) Sources

$$h(y, b; \vec{A}) = \delta_{y_4,t} \sum_{\vec{n}} \delta^3_{\vec{y},2\vec{n}+\vec{A}} \eta(\vec{n}, b) \quad (15)$$

$$\lim_{N\to\infty} \frac{1}{N} \sum_{\eta} \eta(\vec{n}, c)\eta^*(\vec{n}', c') = \delta_{\vec{n},\vec{n}'}\delta_{c,c'} \quad (16)$$

Cubic Wall Sources

$$h(y, b; \vec{A}) = \delta_{y_4,t} \sum_{\vec{n}} \delta^3_{\vec{y},2\vec{n}+\vec{A}} \eta(b) \quad (17)$$

$$\lim_{N\to\infty} \frac{1}{N} \sum_{\eta} \eta(c)\eta^*(c') = \delta_{c,c'} \quad (18)$$

Outline

Fitting Function and Effective Mass

- For staggered fermions, a single-time-slice operator always produces two states, one of which osillates in time.
- In long time separation, the lowest state dominates the correlation function.

Fitting Function

$$C(t) = Z_1 \left[e^{-E_1 t} \pm e^{-E_1 (L-t)} \right] + Z_2 (-1)^t \left[e^{-E_2 t} \pm e^{-E_2 (L-t)} \right], \qquad (19)$$

where L is the lattice size in time-direction. E_1, E_2, Z_1, and Z_2 are fitting parameters.

Effective Mass Plot

- It is important to determine the fitting range $t \in [t_{min}, t_{max}]$ with t_{min} high enough that the lowest mass dominates the correlation function.
- For this purpose, we use the effective mass plots.

Figure: Effective pion mass $(aM_\pi)(\gamma_5 \otimes \gamma_4)$ vs. t for HYP-smeared staggered fermions, cubic U(1) sources (at $t = 0$), and Kluberg-Stern sinks. 370 quenched gauge conf., $\beta = 6$, and $m_1 = m_2 = 0.03$

Effective Mass Plot

- It is important to determine the fitting range $t \in [t_{min}, t_{max}]$ with t_{min} high enough that the lowest mass dominates the correlation function.
- For this purpose, we use the effective mass plots.

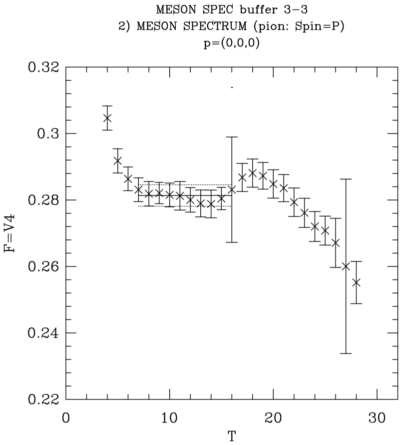

Figure: Effective pion mass $(aM_\pi)(\gamma_5 \otimes \gamma_4)$ vs. t for HYP-smeared staggered fermions, cubic U(1) sources (at $t = 0$), and Kluberg-Stern sinks. 370 quenched gauge conf., $\beta = 6$, and $m_1 = m_2 = 0.03$

Outline

Simulation parameters for quenched study of unimproved staggered fermions

parameters	value
gauge action	Wilson plaquette action
# of sea quarks	0(quenched QCD)
β	6.0
$1/a$	1.95GeV (set by ρ meson mass)
geometry	$16^3 \times 64$
# of confs	$218 \rightarrow 370$
gauge fixing	Coulomb
bare quark mass	$0.005,\ 0.01,\ 0.015,\ 0.02,\ 0.025,\ 0.03$
Z_m	≈ 2.5

Simulation parameters for quenched study of HYP-smeared staggered fermions

parameters	value
gauge action	Wilson plaquette action
# of sea quarks	0(quenched QCD)
β	6.0
$1/a$	1.95GeV (set by ρ meson mass)
geometry	$16^3 \times 64$
# of confs	$218 \rightarrow 370$
gauge fixing	Coulomb
smearing method	HYP (II)
bare quark mass	$0.01, 0.02, 0.03, 0.04, 0.05$
Z_m	≈ 1

Simulation parameters used for the comparison of AsqTad and HYP valence quarks on unquenched configurations

parameters	value
gauge action	1-loop tadpole-improved Symanzik
sea quarks	2+1 flavors of AsqTad staggered
sea quark masses	$am_l = 0.01,\ am_s = 0.05$
β	6.76
a	0.125fm
geometry	$20^3 \times 64$
# of confs	640 (AsqTad) / 406 (HYP)
gauge fixing	Coulomb
valence quark type	AsqTad and HYP staggered
valence quark mass	$(0.007)\, 0.01,\ 0.02,\ 0.03,\ 0.04,\ 0.05$
Z_m	≈ 1

Outline

Unimproved, Quenched, Golterman, Cubic Wall

Figure: $(aM_\pi)^2$vs. aM_q plot using unimproved staggered fermions in quenched QCD with Golterman operators and cubic wall sources.

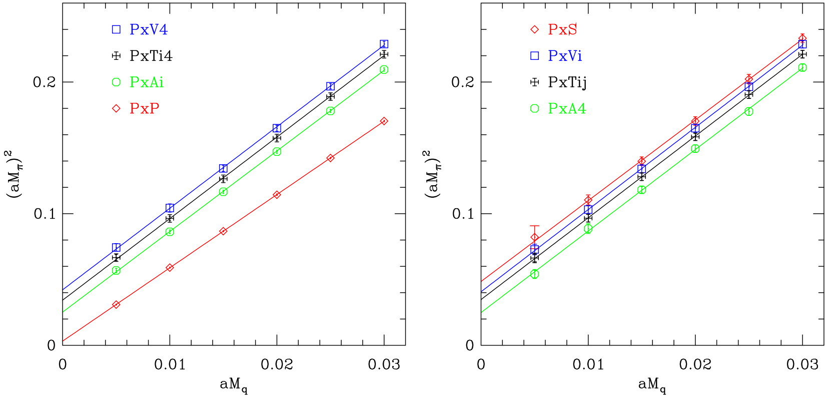

Approximate SO(4) Taste Symmetry

Figure: $(aM_\pi)^2$vs. aM_q plot using unimproved staggered fermions in quenched QCD with Golterman operators and cubic wall sources.

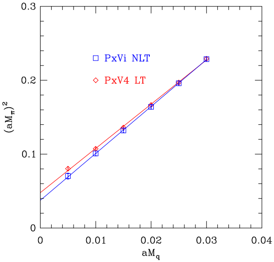

(a) $P \times V_4$ vs. $P \times V_i$

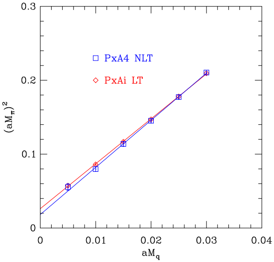

(b) $P \times A_i$ vs. $P \times A_4$

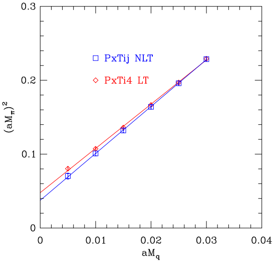

(c) $P \times T_{i4}$ vs. $P \times T_{ij}$

Golterman vs. KS (Unimproved, Quenched, Cubic Wall)

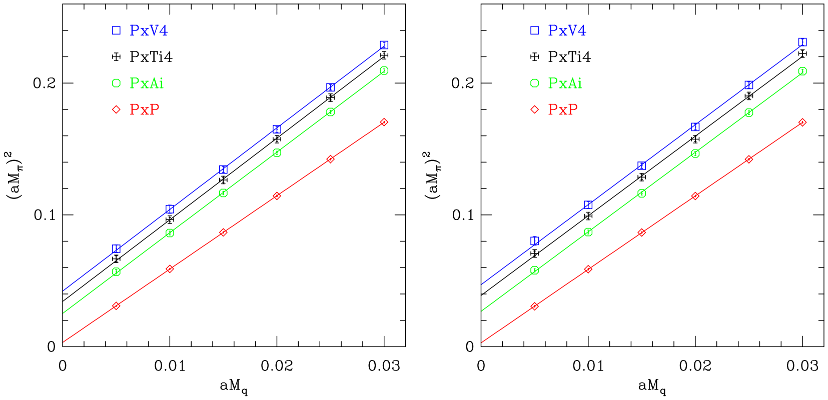

(d) Golterman (e) KS

Golterman vs. KS (Unimproved, Quenched, Cubic Wall)

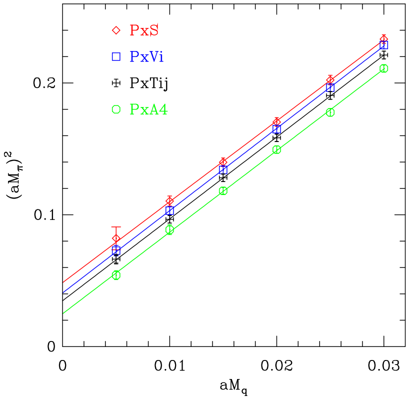

(f) Golterman

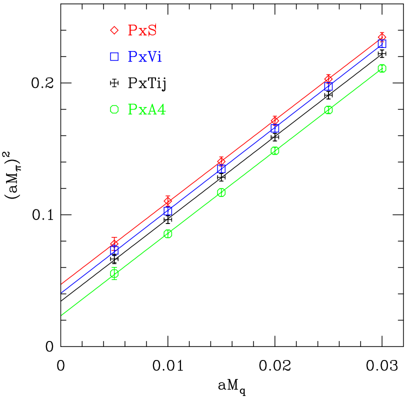

(g) KS

Cubic U(1) vs. Wall (Unimproved, Quenched, Golterman)

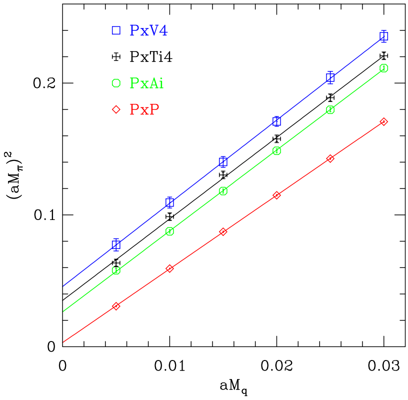

(h) Cubic U(1)

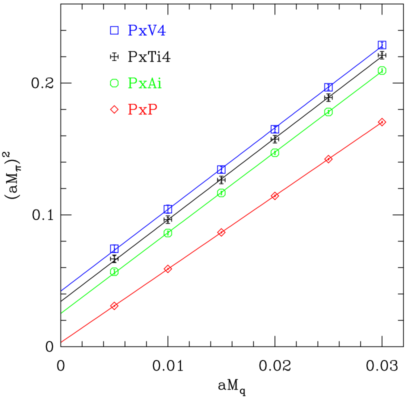

(i) Cubic wall

Cubic U(1) vs. Wall (Unimproved, Quenched, Golterman)

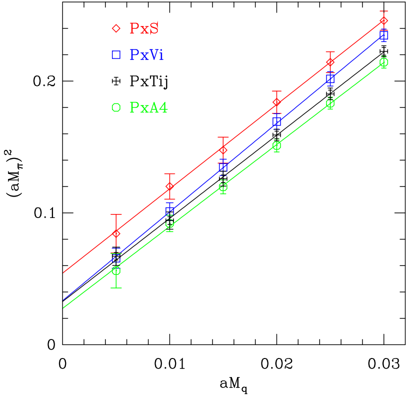

(j) Cubic U(1)

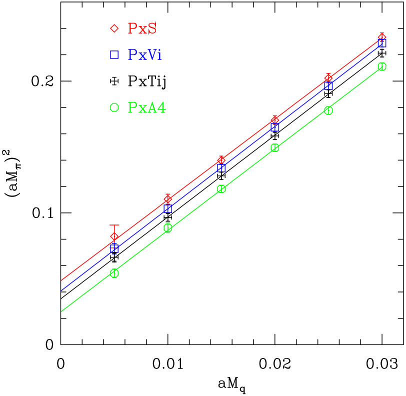

(k) Cubic wall

HYP vs. Unimproved (Quenched, Golterman, Cubic Wall)

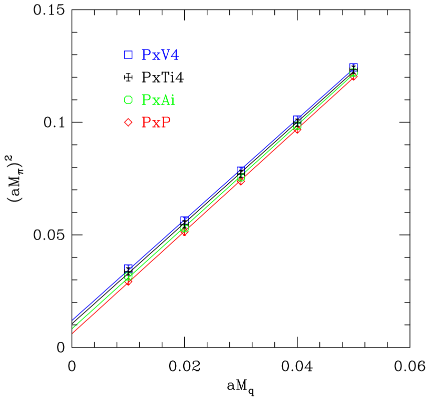

(l) HYP

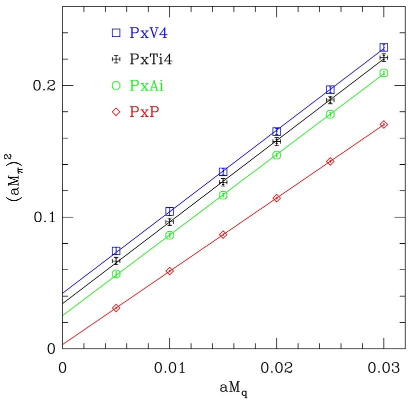

(m) Unimproved

HYP vs. Unimproved (Quenched, Golterman, Cubic Wall)

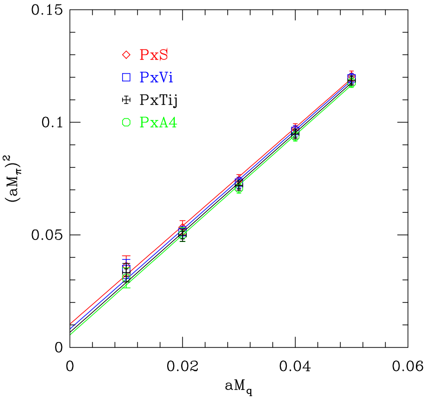

(n) HYP

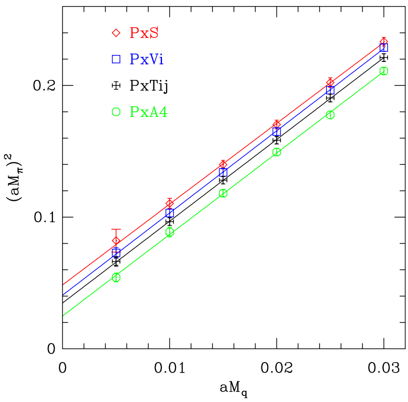

(o) Unimproved

AsqTad vs. HYP in unquenched QCD

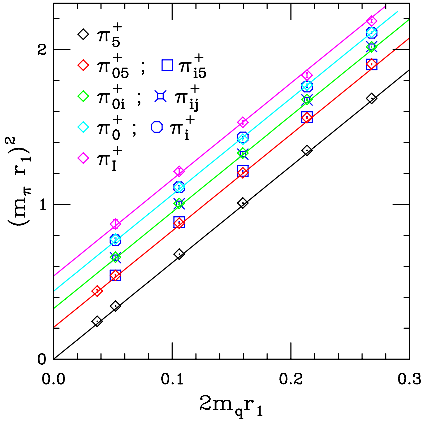

(p) AsqTad (from PRD70(2004)114501)

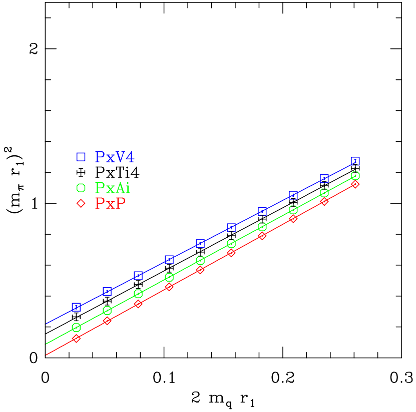

(q) HYP (Golterman, cubic U(1))

AsqTad vs. HYP in unquenched QCD

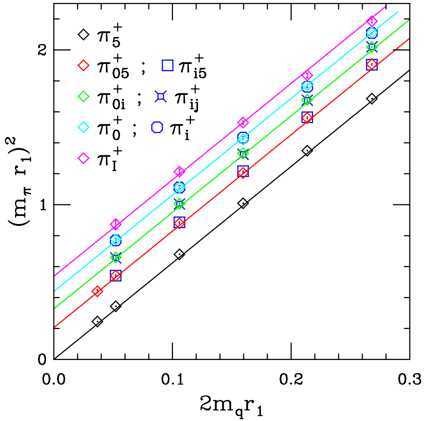

(r) AsqTad (from PRD70(2004)114501)

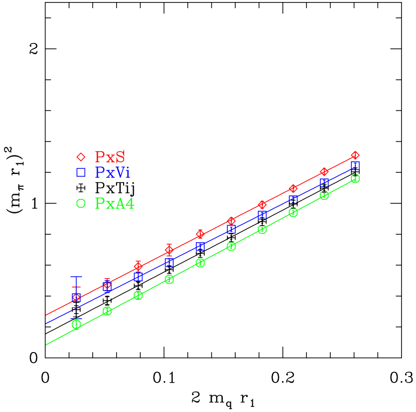

(s) HYP (Golterman, cubic U(1))

AsqTad vs. HYP in unquenched QCD

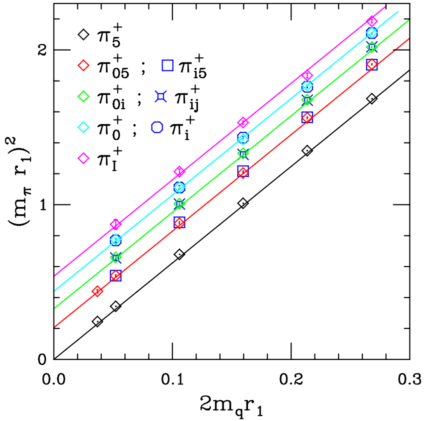

(t) AsqTad (from PRD70(2004)114501)

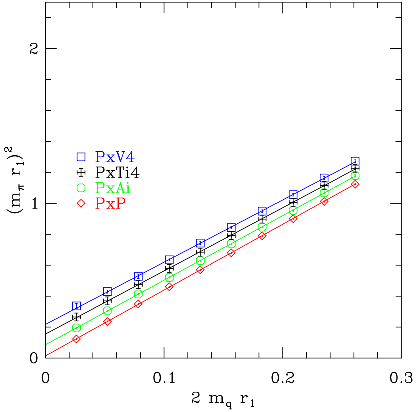

(u) HYP (KS, cubic U(1))

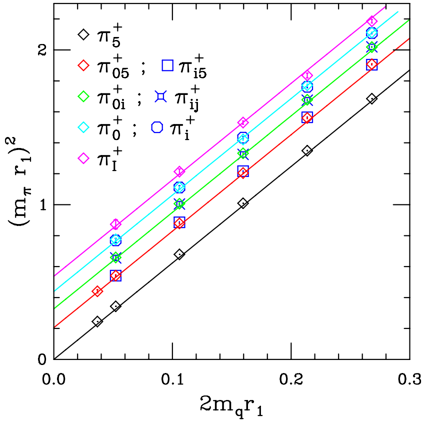

(v) AsqTad (from PRD70(2004)114501)

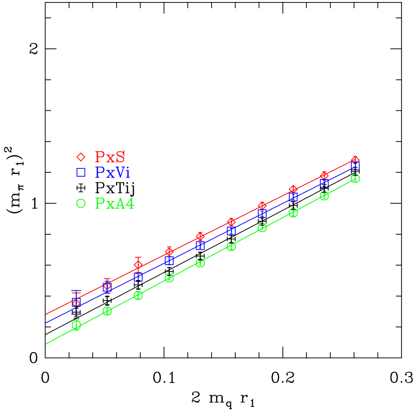

(w) HYP (KS, cubic U(1))

Conclusion

- Cubic wall source is noticeably better than cubic U(1) source.
- No numerical difference between Golterman and KS sink operators.
- HYP-blocking is significantly more efficient in reducing taste-breaking than AsqTad improvement.